

# ChemComm

Accepted Manuscript



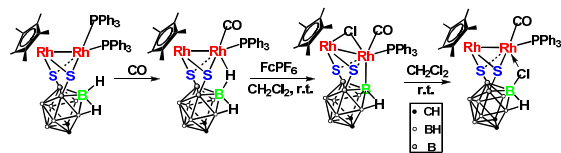
This is an *Accepted Manuscript*, which has been through the Royal Society of Chemistry peer review process and has been accepted for publication.

*Accepted Manuscripts* are published online shortly after acceptance, before technical editing, formatting and proof reading. Using this free service, authors can make their results available to the community, in citable form, before we publish the edited article. We will replace this *Accepted Manuscript* with the edited and formatted *Advance Article* as soon as it is available.

You can find more information about *Accepted Manuscripts* in the [Information for Authors](#).

Please note that technical editing may introduce minor changes to the text and/or graphics, which may alter content. The journal's standard [Terms & Conditions](#) and the [Ethical guidelines](#) still apply. In no event shall the Royal Society of Chemistry be held responsible for any errors or omissions in this *Accepted Manuscript* or any consequences arising from the use of any information it contains.

## Table of Contents



Metal-metal redox synergy is firstly introduced to B-H functionalization of inert dicarba-dodecaboranes under mild conditions in high yields.

## COMMUNICATION

# Metal–Metal Redox Synergy in Selective B–H Activation of *ortho*-Carborane-9,12-dithiolate

Cite this: DOI: 10.1039/x0xx00000x

Xiaolei Zhang, Zhiwen Zhou, Hong Yan\*

Received 00th January 2012,  
Accepted 00th January 2012

DOI: 10.1039/x0xx00000x

www.rsc.org/

**New *o*-carborane-9,12-dithiolate dirhodium complexes are reported to selectively activate inert B–H bonds of *o*-carborane to form B–X bonds by using water, alcohols, alkylhalides (< 60 °C, yields > 80%). Characterization of key intermediates demonstrates oxidative addition and reductive elimination pathway via metal–metal cooperativity.**

Carboranes have been used for decades in pharmaceuticals, materials and catalysis.<sup>1–3</sup> Functionalization of B–H bonds<sup>4</sup> is an important strategy for rapid generation of versatile carborane derivatives to enable these diverse applications. Metal-mediated hydroboration of carboranes have been reported as an important method for direct cage boron derivatization.<sup>4,5</sup> In view of the spectacular role of metals in functionalization of B–H bond, M–B bond formation is involved.<sup>4–6</sup> Note that B–H activation of small boranes<sup>7</sup> has been successful in which metal–boryl complexes serve as intermediates in C–H borylation. However, selective B–H activation of carboranes leading to B–H functionalization via a M–B bond is still challenging. To date, the scopes of substrates that are able to achieve B–H activation as well as further chemical transformations of intermediates containing a M–B bond represent major problems in the use of a single metal.<sup>4–6</sup>

Another strategy for B–H activation of carboranes is to use cooperative metal–metal (M–M) interactions inspired by Nature's highly efficient redox machinery on the basis of polynuclear active sites.<sup>8</sup> Thus, it is anticipated that metal–metal redox synergy may lower the energy barrier for the redox pathway of B–H activation and boron–heteroatom bond formation in comparison to single metal-mediated system.<sup>4–6</sup> However, examples for B–H activation at carboranes utilizing bimetallic redox synergy is not known. In the case of analogous C–H activation, the redox pathway at a single metal center has been well-established,<sup>9</sup> but the studies on the redox pathway at a two-metal model system is still rare<sup>10</sup>. For example, Ritter *et al* described bimetallic palladium complexes that can lower the energy barrier for C–H functionalization.<sup>10a</sup> Mankad *et al* reported C–H borylation utilizing bimetallic Cu–Fe/Zn–Fe cooperativity.<sup>10b</sup> Nevertheless, both examples involved metal–metal bond cleavage pathway in bimetallic redox cooperation owing to the orbital symmetry inhibition (Chart 1).<sup>10c</sup>

To evaluate the role of metal–metal redox synergy in B–H activation of inert carboranes, here, we report selective B–H activation and the further B–Cl and B–O bond formation in the *o*-carborane-9,12-dithiolate dirhodium complexes by using the common substrates such as CH<sub>2</sub>Cl<sub>2</sub>, CHCl<sub>3</sub>, methanol and water. The characterization of new dirhodium complexes bearing Rh–H–B, Rh–B, Rh–H–Rh and Rh–Cl–Rh bonds has provided valuable mechanistic evidences on B–H activation through metal–metal redox synergy with unconventional variable metal–metal bond order in contrast to the metal–metal bond cleavage pathway (Chart 1).

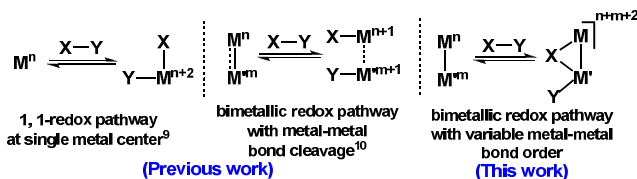


**Chart 1.** Illustration of redox pathways at single- and two-metal centers.

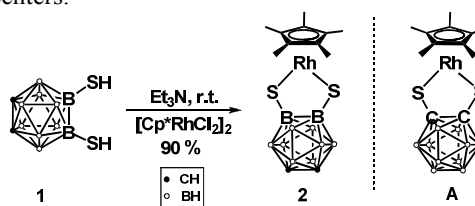
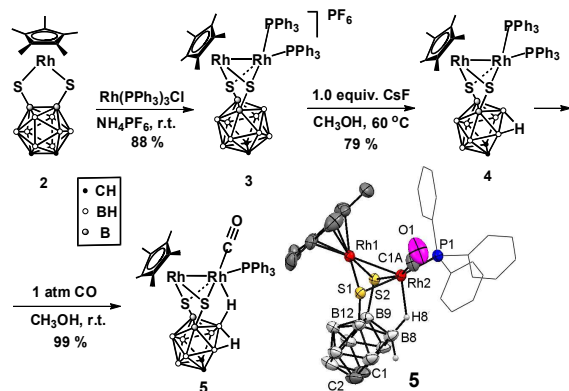


**Fig. 1** (a) Synthesis of boron-substituted 16e complex **2** from *o*-carborane-9,12-dithiol (**1**) and schematic comparison of its structural analogous complex **A**.

*o*-Carborane-9,12-dithiol (**1**)<sup>11</sup> is suited for construction of 16e half sandwich complex **2**, analogous to previously well reported complex **A** [Cp<sup>\*</sup>Rh{1,2-S<sub>2</sub>C<sub>2</sub>(B<sub>10</sub>H<sub>10</sub>)}]<sup>12</sup> (Cp<sup>\*</sup> = η<sup>5</sup>-C<sub>5</sub>Me<sub>5</sub>) (Fig. 1) prepared from *o*-carborane-1,2-dithiol. Complex **A** has been widely used as synthon<sup>3d,5</sup> that easily led to B–H activation at B(3)/B(6).<sup>5</sup> The analogous structure of **2** with S–B rather than S–C in **A**, however, shows different reaction chemistry at the Rh–S bonds that does not lead to B–H activation (SI-Scheme S1) likely due to the increased electron charge density at the sulfur atoms from the electron-donating carboranyl group.<sup>13</sup>



**Scheme 1.** Synthetic route to di-rhodium complexes bearing *o*-carborane-9,12-dithiolate ligand and molecular structure of **5**.

Thus dirhodium complexes were prepared, as shown in Scheme 1, to test the ability to induce B–H bond activation. After consideration of orbital symmetry inhibition<sup>10c</sup> in bimetallic redox pathways, Rh(PPh<sub>3</sub>)<sub>3</sub>Cl was selected to react with **2** in the presence of NH<sub>4</sub>PF<sub>6</sub> to give rise to dinuclear complex **3** (SI-Fig. S2). Deboronation of **3** under basic conditions afforded neutral complex **4** containing a *nido*-carborane unit (SI-Fig. S3). Both complexes **3** and **4** are stable in solid state but the Rh–PPh<sub>3</sub> bond is labile in solution, as reported in literature.<sup>14</sup> To evaluate the interaction between the B–H bond and metal centers, one bulky PPh<sub>3</sub> was replaced by CO, as a result, the carbonyl product **5** containing a Rh–H–B bond was generated in a quantitative yield (Scheme 1). The Rh2–H8 distance in **5** (2.075 Å) is much shorter than that (2.714 Å, SI-Fig. S3 and S4) in **4**, suggesting a strong interaction between the B–H bond and the Rh center in **5**. In solution the <sup>1</sup>H {<sup>11</sup>B} NMR spectrum shows the characteristic broad peak of Rh–H–B at –1.21 ppm consistent with the data in the known species bearing Rh–H–B bond.<sup>4d</sup> Correspondingly, the <sup>11</sup>B signal of Rh–H–B is significantly low-frequency shifted (> 5 ppm) in comparison to that in **4**. This gives an excellent example of the effect of steric factors on B–H activation.

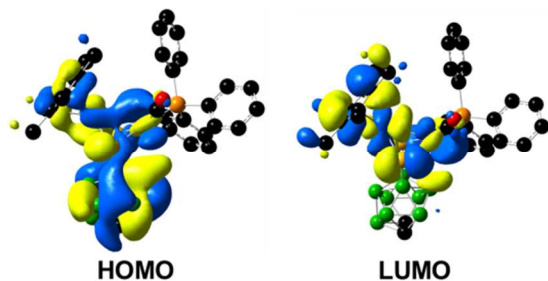
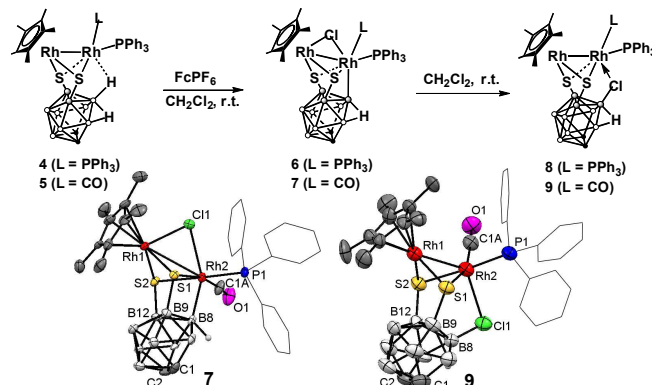


**Fig. 2** Calculated molecular orbitals of **5** at B3PW91/6-31G(d, p)/LANL2DZ [Rh] level. The HOMO illustrated the Rh–Rh bonding orbitals whereas the LUMO exhibited the anti-bonding orbitals.

Structural determination of complex **5** provides a convincing model for calculating the bonding nature of Rh–H–B bond by DFT study. In Fig. 2, the HOMO (Highest Occupied Molecular Orbital) confirms the Rh–Rh binding in a non-symmetric fashion. The LUMO (Lowest Unoccupied Molecular Orbital) is mainly located at the metal cluster (73 %) and Cp\* ring (22 %) but the orbital contribution of B(8)–H bond is not negligible (5 %). This predicts the potential nucleophilic attack of metal center toward the boron atom.



**Scheme 2.** B–H bond activation and B–Cl bond reductive elimination in the dirhodium complexes.

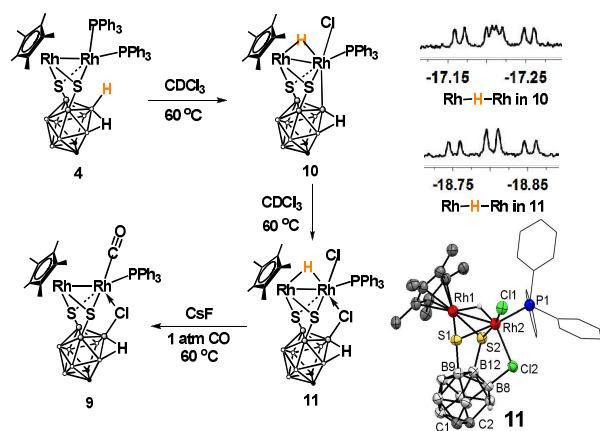
Treatment of complex **4** or **5** with 1.0 equiv. of FcPF<sub>6</sub> in CH<sub>2</sub>Cl<sub>2</sub> at ambient temperature led to complex **6** or **7** which contains a Rh–B bond (Scheme 2, SI-Fig.S7). This demonstrates that the B–H bonds have been activated in both complexes in the presence of an oxidant and a chlorine source. The <sup>11</sup>B NMR resonances of the Rh–B units (–36.8 ppm in **6** and –39.7 ppm in **7**) have been further low-frequency shifted (5 to 7 ppm) relative to those in **4** and **5**. The solid-state structure of **7** exhibits a Rh–B bond (2.129 Å) and a Rh–Cl–Rh bond with extremely long Rh–Rh distance (3.157 Å, Scheme 2), in comparison to the Rh–Rh distances (2.584 to 3.232 Å) in known Rh–Cl–Rh species.<sup>15</sup>

The reductive elimination of **6** and **7** at ambient temperature yielded products **8** and **9** (Scheme 2), respectively, in high yields (> 80%) which contain a B–Cl bond and a normal Rh–Rh bond (2.739 Å for **8** and 2.688 Å for **9**, SI-Fig. S8 and S9), as confirmed by the X-ray structures. The <sup>11</sup>B NMR signals of B–Cl appear around 5.0 ppm in **8** and **9**, dramatically shifted to high frequency by over 40 ppm vs. those of the Rh–B bonds in **6** and **7**, further confirming B–Cl reductive elimination at the dirhodium centers. Note that other alkyl chlorides such as CHCl<sub>3</sub>, ClCH<sub>2</sub>CH<sub>2</sub>Cl and PhCH<sub>2</sub>Cl also react similarly. A radical pathway for chlorine abstraction<sup>16</sup> may be involved as addition of Cl<sup>–</sup> source (*n*-Bu<sub>4</sub>NCl or HCl<sub>(aq)</sub>) only led to decomposition of **4** or **5**.

**Table 1.** Listed Rh–Rh distances and WBI (Wiberg bond indices) values for **5**, **7**, **9** and **11**.

complex	<b>5</b>	<b>7</b>	<b>9</b>	<b>11</b>
Rh–Rh/Å (cry.)	2.7274(11)	3.1566(5)	2.6878(4)	2.6946(4)
Rh–Rh/Å (cal.)	2.773	3.228	2.716	2.722
WBI values	0.3054	0.0655	0.3517	0.2464

This is a standard sequence to demonstrate two-metal mediated B–H activation through adjusting Rh–Rh distance which is restored after B–Cl reductive elimination. To gain insights into electronic structure, a DFT calculation of complex **7** has been conducted which supports the low orbital symmetry in the Rh–Cl–Rh bonding scheme (SI-Fig. S24). The Wiberg bond indices (WBI) values were calculated for the Rh–Rh bond order and found to be 0.0655 in contrast to the much stronger Rh–Rh interactions in the precursor **5** (0.3054) and the product **9** (0.3517) (Table 1). Both structural determinations and theoretical calculations provide persuasive bond order support for reductive elimination from dimetal centers involving variable metal–metal bond order. This represents an unconventional metal–metal redox pathway in contrast to the metal–metal bond cleavage pathway<sup>10a,b</sup> in bimetallic redox chemistry (Chart 1).



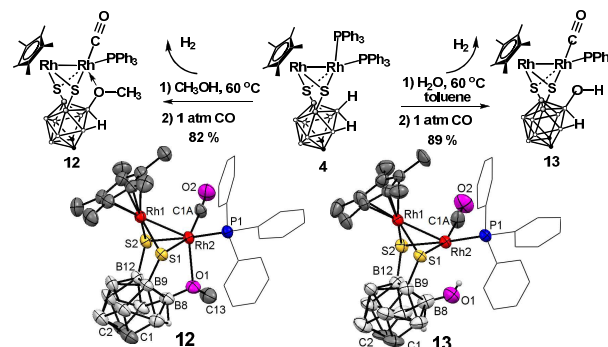
**Scheme 3.** Reactivity of complex **4** towards  $\text{CDCl}_3$  at  $60^\circ\text{C}$ .

Above results demonstrate that an external oxidant (i.e.  $\text{FcPF}_6$ ) facilitates B–H activation which occurs rapidly at room temperature. To better understand B–H activation at the very initial stages, complex **4** was heated in  $\text{CDCl}_3$  at  $60^\circ\text{C}$  without addition of oxidant (Scheme 3) and this process was monitored by NMR and HRMS (SI-Fig. S13–16). The expected earlier intermediate bearing a Rh–H–B bond ( $\delta = -3.69$  ppm in  $^1\text{H}$  { $^{11}\text{B}$ } NMR) was detected in the first two hours (species **B** in SI-Fig. S11). Furthermore, complex **10** having both Rh–B and Rh–H–Rh bonds was observed which has a characteristic multiple hydride resonance ( $^1J_{\text{Rh1-H}} = 20$  Hz,  $^1J_{\text{Rh2-H}} = 20$  Hz,  $^2J_{\text{P-H}} = 10$  Hz) (Scheme 3). The Rh–B formation was confirmed by a distinctive low-frequency  $^{11}\text{B}$  NMR signal at  $-40.3$  ppm compared to the signals for B–H ( $-10.2$  to  $-28.6$  ppm) in **4**. The ESI-HRMS spectrum shows its molecular ion peak at  $834.1007$  for  $[\text{M}+\text{H}]^+$  (SI-Fig. S16). The short life of **10** does not allow an additional structural characterization, but the spectral data is sufficient to state that B–H oxidative addition to di-rhodium centers has occurred. Complex **10** can cleanly convert to a new product **11** within 12 h in refluxing  $\text{CDCl}_3$  (SI-Fig. S12 and S13). The hydride signal, a doublet of triplets at  $-18.80$  ppm with  $^1J_{\text{Rh-H}} = 20$  Hz,  $^2J_{\text{P-H}} = 10$  Hz is typical of a bridging Rh–H–Rh bond (Scheme 3). The  $^{11}\text{B}$  NMR signal of B–Cl ( $5.2$  ppm) is shifted to high frequency by around  $45$  ppm vs Rh–B ( $-40.3$  ppm) in **10**. In solid state, the bridging hydride between Rh–Rh bond (Rh1–Rh2  $2.695$  Å, Rh–H  $1.2921$  and  $1.7324$  Å, Scheme 3, SI-Fig. S10) was identified by the electron density difference map.

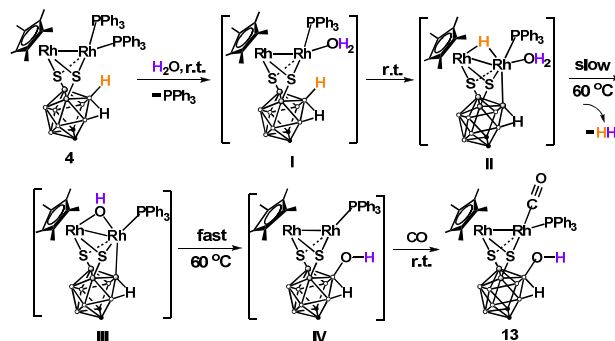
The above results demonstrate the putative intermediate in di-rhodium mediated B–H activation to be species **10** containing a Rh–H–Rh bond, which is different from the conventional terminal hydride invoked in single-metal mediated<sup>4c,7c</sup> oxidative addition of a B–H bond. In general, the latter is more reactive. A Nature Bonding Orbital (NBO) analysis of **11** exhibits lower Rh–Rh bond order but shorter Rh–Rh bond length compared to **5** and **9** (Table 1). This indicates that the Rh–H–Rh bond possesses more anti-bonding character vs the conventional Rh–Rh bond, predicting the potential reactivity. Indeed, addition of carbon monoxide and  $\text{CsF}$  to **11** has led to product **9** (Scheme 3).

To further understand the role of metal–metal redox synergy in B–H activation, the reactivity of **4** was examined toward other substrates such as  $\text{CH}_3\text{OH}$  and water. The reaction of **4** and  $\text{CH}_3\text{OH}$  or water at  $60^\circ\text{C}$  followed by bubbling  $\text{CO}$  afforded **12** (82%) or **13** (89%), respectively (Scheme 4). Both structures feature a B–O bond ( $1.411$  Å in **12**, and  $1.424$  Å in **13**, Scheme 4, SI-Fig. S11 and S12). The different electronic effects of methyl and hydrogen lead to

different coordination fashion as indicated by Rh2...O1 distances in **12** ( $2.470$  Å) and **13** ( $2.709$  Å). The  $^{11}\text{B}$  NMR signals of B–O have high-frequency shifted to  $5.8$  ppm in **12** and  $4.4$  ppm in **13** relative to  $-10.2$  to  $-28.6$  ppm for B–H in **4**. The formation of B–O bond in **13** demonstrates activation of both the inert B–H bond of carborane and the O–H bond of water under mild conditions has been achieved. This result should be attributed to the intriguing role of Rh–Rh redox synergy to lower energy barrier since direct B–O coupling between carborane and water has not been achieved by a single metal.



**Scheme 4.** Reactivity of complex **4** toward methanol and water.



**Scheme 5.** Proposed mechanism for the formation of B–O bond via activating both B–H bond of carborane and O–H bond of water.

To better understand this process, the reaction of **4** and  $\text{H}_2\text{O}$  was studied through monitoring by NMR and HRMS (for details, see SI-Section 4). As shown in Scheme 5, we propose that the reaction starts from ligand substitution of  $\text{PPh}_3$  by  $\text{H}_2\text{O}$  (**I**) to initiate B–H oxidative addition (**II**) at ambient temperature, as occurred from **4** to **5** after release of bulky  $\text{PPh}_3$ . The formation of Rh–H–Rh hydride and Rh–B bond in **II** was detected by  $^1\text{H}$  and  $^{11}\text{B}$  NMR (SI-Fig. S17 and S19). The molecular ion peak of **I** and **II** was observed by HRMS to indicate the presence of the coordinate  $\text{H}_2\text{O}$  (SI-Fig. S18 and SI-Table S1). Then at an elevated temperature  $\text{H}_2$  is released, followed by formation of **III**. Although this species was not observed by NMR probably owing to the short life, hydroxo-bridged dirhodium complexes derived from reactions of water and rhodium compounds have been described.<sup>17</sup> The generation of  $\text{H}_2$  was confirmed by GC (SI-Fig. S21). Finally, B–O reductive elimination occurs to form **IV** which is stable and has been characterized by NMR and HRMS (SI-Fig. S19 and S20). Addition of  $\text{CO}$  leads to isolatable product **13**. Notably, water has been used as a clean oxygen or hydrogen supplier mediated by organometallic complexes,<sup>18</sup> however, dehydrogenative B–O coupling of carborane using water with release of  $\text{H}_2$  is not known. In addition, hydroxylation and chlorination of polyhedral boranes have been reported,<sup>19</sup> however, those

methods required demanding reaction conditions ( $\text{H}_2\text{O}_2/100\text{ }^\circ\text{C}$  or N-chloimide/AcOH/ $150\text{ }^\circ\text{C}$ ) and tedious procedures. Here the new dinuclear metal-mediated B–H activation provides a promising approach to both B–Cl and B–O formation under mild conditions by using common substrates.

## Conclusions

In conclusion, a new type of dirhodium complexes containing boron-substituted *nido-o*-carborane dithiolate has been developed. These complexes are able to selectively activate B–H bond at the B8 site of carborane and allow further functionalization to form B–Cl or B–O bond under mild conditions ( $<60\text{ }^\circ\text{C}$ ) in isolated yields of over 80%. Characterization of both in-situ generated and isolated intermediate species containing Rh–H–B, Rh–B, Rh–H–Rh and Rh–Cl–Rh bonds strongly demonstrates metal–metal redox synergy in B–H functionalization in contrast to the reported single metal-induced B–H activation at B(3)/B(6) sites that usually led to B–C formation with yields of less than 50% owing to the presence of parallel pathways.<sup>5</sup> The mechanism of dehydrogenative B–O coupling between water and carborane also support metal–metal redox synergy. This work opens a door to efficient synthesis of carborane-functionalized derivatives at B(8) site.

We thank the National Basic Research Program of China (2010CB923303 and 2013CB922101) and the National Science Foundation of China (21271102). We are grateful to the High Performance Computing Center of Nanjing University.

## Notes and references

State Key Laboratory of Coordination Chemistry, School of Chemistry and Chemical Engineering, Nanjing University, Nanjing, Jiangsu 210093 (China). Fax: (+86)25-83314502, E-mail: hyan1965@nju.edu.cn.

Electronic Supplementary Information (ESI) available: [Complete experimental procedures, spectral data for new compounds, calculation details and crystallographic data (CIF)]. See DOI: 10.1039/b000000x/

- (a) N. S. Hosmane, *Boron Science: New Technologies and Applications*; CRC Press: Boca Raton, FL, 2011; (b) R. N. Grimes, *Carboranes* 2nd edition (Elsevier, 2011); (c) M. F. Hawthorne, *Angew. Chem. Int. Ed.* 1993, **32**, 950; (d) V. I. Bregadze, I. B. Sivaev, S. A. Glazun, *Anti-Cancer Agents Med. Chem.* 2006, **6**, 75; (e) J. Plešek, *Chem. Rev.* 1992, **92**, 269; (f) V. I. Bregadze, *Chem. Rev.* 1992, **92**, 209.
- (a) B. P. Dash, R. Satapathy, E. R. Gaillard, J. A. Maguire, N. S. Hosmane, *J. Am. Chem. Soc.* 2010, **132**, 6578; (b) K. R. Wee, Y. J. Cho, J. K. Song, S. O. Kang, *Angew. Chem., Int. Ed.* 2013, **52**, 9682; (c) C. Shi, H. Sun, X. Tang, H. Lv, H. Yan, Q. Zhao, J. Wang, W. Huang, *Angew. Chem., Int. Ed.* 2013, **52**, 13434; (d) C. Masalles, J. Llop, F. Teixidor, *Adv. Mater.* 2002, **14**, 826; (e) K. Kokado, Y. Tokoro and Y. Chujo, *Macromolecules*, 2009, **42**, 2925; (f) M. Tominaga, Y. Morisaki, Y. Chujo, *Macromol. Rapid Commun.* 2013, **34**, 1357; (g) L. Weber, J. Kahlert, R. Brockhine, L. Böhlting, A. Brockhike, H. Stammier, B. Neumann, R. A. Harder, M. A. Fox, *Chem. Eur. J.* 2012, **18**, 8347.
- (a) N. S. Hosmane, J. A. Maguire, In *Comprehensive Organometallic Chemistry III*; R. H. Crabtree and D. M. P. Mingos, Eds.; Elsevier: Oxford, 2007; Vol. 3, Chapter 5; (b) Z. Xie, *Acc. Chem. Res.* 2003, **36**, 1; (c) S. Liu, Y. F. Han, G. X. Jin, *Chem. Soc. Rev.* 2007, **36**, 1543; (d) Z. Qiu, S. Ren, Z. Xie, *Acc. Chem. Res.* 2011, **44**, 299.
- (a) E. W. Corcoran, L. G. Sneddon, In *Advances in Boron and the Boranes*; J. F. Liebman, A. Greenberg, R. E. Williams, Eds.; VCH: New York, 1988, p 71; (b) D. Olid, R. Núñez, C. Viñas, F. Teixidor, *Chem. Soc. Rev.* 2013, **42**, 3318; (c) J. D. Hewes, C. W. Kreimendahl, T. B. Marder, M. F. Hawthorne, *J. Am. Chem. Soc.* 1984, **106**, 5757; (d) E. Molinos, G. Kociok-Kohn, A. S. Weller, *Chem. Comm.* 2005, 3609.
- (a) M. Herberhold, H. Yan, W. Milius, B. Wrackmeyer, *Angew. Chem., Int. Ed.* 1999, **38**, 3689; (b) R. Zhang, L. Zhu, G. Liu, H. Dai, Z. Lu, J. Zhao, H. Yan, *J. Am. Chem. Soc.* 2012, **134**, 10341; (c) Z. J. Wang, H. D. Ye, Y. G. Li, Y. Z. Li, H. Yan, *J. Am. Chem. Soc.* 2013, **135**, 11289; (d) M. Herberhold, H. Yan, W. Milius, B. Wrackmeyer, *Chem. Eur. J.* 2002, **8**, 388.
- (a) M. Liu, L. Dang, Z. Y. Lin, Z. W. Xie, *J. Am. Chem. Soc.* 2008, **130**, 16103; (b) Z. J. Yao, W. B. Yu, Y. J. Lin, S. L. Huang, Z. H. Li, G. X. Jin, *J. Am. Chem. Soc.* 2014, **136**, 2825; (c) A. M. Spokoyny, M. G. Reuter, C. L. Stern, M. A. Ratner, T. Seideman, C. A. Mirkin, *J. Am. Chem. Soc.* 2009, **131**, 9482.
- (a) H. Y. Chen, S. Schlecht, T. C. Semple, J. F. Hartwig, *Science* 2000, **287**, 1992; (b) J. Y. Cho, M. K. Tse, D. Holmes, R. E. Maleczka, M. R. Smith, *Science* 2002, **295**, 305; (c) S. Shimada, A. S. Batsanov, J. A. K. Howard, T. B. Marder, *Angew. Chem. Int. Ed.* 2001, **40**, 2168; (d) I. A. I. Mkhallid, J. H. Barnard, T. B. Marder, J. M. Murphy, J. F. Hartwig, *Chem. Rev.* 2010, **110**, 890.
- (a) B. M. Hoffman, D. R. Dean, L. C. Seefeldt, *Acc. Chem. Res.* 2009, **42**, 609; (b) M. J. Corr, J. A. Murphy, *Chem. Soc. Rev.* 2011, **40**, 2279.
- For reviews, see: (a) *Chem. Rev.* 2010, **110**, 575-1211, Issue name: selective functionalization of C–H bonds.
- (a) D. C. Powers, T. Ritter, *Acc. Chem. Res.* 2012, **45**, 840; (b) T. J. Mazzacano, N. P. Mankad, *J. Am. Chem. Soc.* 2013, **135**, 17258; (c) G. Trinquier, R. Hoffmann, *Organometallics* 1984, **3**, 370; (d) T. G. Gray, A. S. Veige, D. G. Nocera, *J. Am. Chem. Soc.* 2004, **126**, 9760; (e) M. R. Radlauer, M. W. Day, T. Agapie, *J. Am. Chem. Soc.* 2012, **134**, 1478; (f) S. A. Reed, M. C. White, *J. Am. Chem. Soc.* 2008, **130**, 3316.
- J. Plešek, Z. Janoušek, S. Heřmánek, *Coll. Czech. Chem. Comm.* 1980, **45**, 1775.
- M. Herberhold, H. Yan, W. Milius, B. Wrackmeyer, *J. Organomet. Chem.* 1999, **587**, 252.
- (a) A. M. Spokoyny, C. W. Machan, D. C. Clingerman, M. S. Rosen, M. J. Wiester, R. D. Kennedy, A. A. Sarjeant, C. L. Stern, C. A. Mirkin, *Nat. Chem.* 2011, **3**, 590; (b) X. L. Zhang, X. Tang, J. Yang, Y. Li, H. Yan, V. I. Bregadze, *Organometallics* 2013, **32**, 2014.
- R. H. Crabtree, *The Organometallic Chemistry of the Transition Metals (4th Edition ed.)*, 2005, Chapter 4.
- (a) G. H. Chen, J. Y. Gui, L. C. Li, J. Liao, *Angew. Chem., Int. Ed.* 2011, **50**, 7681; (b) Z. Freixa, P. C. Kamer, M. Lutz, A. L. Spek, P. W. N. M. Leeuwen, *Angew. Chem., Int. Ed.* 2005, **44**, 4385.
- (a) H. R. Dias, R. G. Browning, S. A. Polach, H. V. Diyabalanage, C. J. Lovely, *J. Am. Chem. Soc.* 2003, **125**, 9270; (b) Z. Csok, O. Vechorkin, S. B. Harkins, R. Scopelliti, X. Hu, *J. Am. Chem. Soc.* 2008, **130**, 8156; (c) J. Breitenfeld, J. Ruiz, M. D. Wodrich, X. L. Hu, *J. Am. Chem. Soc.* 2013, **135**, 12004.
- (a) F. Christensson, J. Springborg, *Inorg. Chem.* 1985, **24**, 2129; (b) A. Drljaca, A. Zahl, R. V. Eldik, *Inorg. Chem.* 1998, **37**, 3948.
- (a) E. Balaraman, E. Khaskin, G. Leitius, D. Milstein, *Nat. Chem.* 2013, **5**, 123; (b) X. F. Fu, S. Li, B. B. Wayland, *J. Am. Chem. Soc.* 2006, **128**, 8947; (c) C. T. To, K. S. Choi, K. S. Chan, *J. Am. Chem. Soc.* 2012, **134**, 11388.
- (a) T. Peymann, A. Herzog, C. B. Knobler, M. F. Hawthorne, *Angew. Chem., Int. Ed.* 1999, **38**, 1062; (b) O. V. Alekseenko, S. N. Dugin, E. L. Gurova, P. A. Storozhenko, RU2454422, 2012-06-27; (c) K. C. Kim, C. A. Reed, G. S. Long, A. Sen, *J. Am. Chem. Soc.* 2002, **124**, 7662.